

# Effective nonlocal spin injection through low-resistance oxide junctions



Yunjiao Cai <sup>a,\*</sup>, Yongming Luo <sup>b,c</sup>, Chuan Qin <sup>a</sup>, Shuhan Chen <sup>a</sup>, Yizheng Wu <sup>b</sup>, Yi Ji <sup>a</sup>

<sup>a</sup> Department of Physics and Astronomy, University of Delaware, Newark, Delaware 19716, USA

<sup>b</sup> State Key Laboratory of Surface Physics and Department of Physics, Fudan University, Shanghai 200433, PR China

<sup>c</sup> Center for Integrated Spintronic Devices, Hangzhou Dianzi University, Hangzhou, Zhejiang 310018, PR China

## ARTICLE INFO

### Article history:

Received 11 February 2015

Received in revised form

8 December 2015

Accepted 16 December 2015

Available online 19 December 2015

### Keywords:

Spin injection

Nonlocal spin valve

Pure spin current

Spin transport

Nonlocal spin polarization

Low-resistance oxide junction

## ABSTRACT

Many ( $> 40$ ) nonlocal spin valves on the same substrate have been characterized at 6 K and 295 K by using a probe station. Low-resistance oxide junctions ( $0.2\text{--}0.8\ \Omega$ ) are used to inject spin current into mesoscopic Cu channels. Spin signals exceeding  $10\ \text{m}\Omega$  at 6 K have been consistently observed, indicating efficient spin injection and detection. However, complex switching behavior and possible variations between devices pose a challenge to using a standard fitting method to quantify the spin signals. Two methods are used for quantitative analysis. The range of the effective spin polarizations can be estimated by assuming a reasonable range for the Cu spin diffusion lengths. A nonlocal spin polarization is introduced to evaluate the spin current in the Cu channels.

© 2015 Elsevier B.V. All rights reserved.

## 1. Introduction

Nonlocal spin valves (NLSV), [1–3] also known as lateral spin valves, are devices in which pure spin currents are generated in nonmagnetic channels made of metals, [3] semiconductors, [4–6] or graphene. [7] They have the unique trait that a pure spin current can be transported across a lateral distance of micrometers on a substrate and remain detectable. The pure spin current in metallic NLSVs has been used to achieve inverse and direct spin Hall effects [8,9] and spin Seebeck effects. [10] The spin relaxation in the metallic nonmagnetic channels has prompted interesting studies. [11–15] Metallic NLSV devices have been proposed as read-head sensors for high-density magnetic recordings. [16] In light of the growing interest in metal-based magnetic memory and logic devices, the pursuit of high-quality metallic NLSVs is desirable.

In this work, we demonstrate effective nonlocal spin injection through low-resistance aluminum oxide ( $\text{AlO}_x$ ) junctions. The area of the junctions is  $330 \times 170\ \text{nm}^2$ , and the resistance is estimated to be  $0.2\text{--}0.8\ \Omega$ . An array of such NLSV structures is fabricated on the same substrate, and more than 40 devices are characterized by a variable temperature probe station. Despite the low resistance of the junctions, large spin signals are observed at 295 K and 6 K,

indicating efficient spin injection and transport. Quantifying the results using the standard fitting methods poses challenges, however, because of the complex switching behaviors and the possible variations in properties from one device to another. We can estimate the range of the effective spin injection (detection) polarizations by assuming a reasonable range for the Cu spin diffusion lengths. The spin current in the Cu channel can also be quantified with a nonlocal spin polarization.

## 2. Experiments

We fabricated 400  $\text{Py}/\text{AlO}_x/\text{Cu}$  NLSV devices and arranged them in a  $20 \times 20$  matrix within a  $6 \times 6\ \text{mm}^2$  area on a  $10 \times 10\ \text{mm}^2$  silicon substrate during a single fabrication batch. Fig. 1(a) shows a scanning electron microscope (SEM) image of a single device. The structure is formed by electron beam lithography followed by a shadow evaporation process. [3,13,17,18] Two Py (permalloy or  $\text{Ni}_{81}\text{Fe}_{19}$  alloy) pads  $330\ \text{nm}$  wide are used as the spin injector ( $F_1$ ) and the spin detector ( $F_2$ ). The thicknesses of  $F_1$  and  $F_2$  are  $31\ \text{nm}$  and  $15\ \text{nm}$  respectively. The center-to-center distance ( $L$ ) between  $F_1$  and  $F_2$  ranges from  $400\ \text{nm}$  to  $700\ \text{nm}$ . The Cu channel is  $110\ \text{nm}$  thick and  $160\text{--}180\ \text{nm}$  wide. A layer of  $3\ \text{nm}\ \text{AlO}_x$  is directly evaporated between Py and Cu, forming  $\text{Py}/\text{AlO}_x/\text{Cu}$  junctions with an average area of  $330 \times 170\ \text{nm}^2$ .

Using cross-junctions, the resistance–area ( $RA$ ) product of the  $\text{Py}/\text{AlO}_x/\text{Cu}$  barriers is measured with a four-probe method to be

\* Corresponding author.

E-mail addresses: [yjcai@udel.edu](mailto:yjcai@udel.edu) (Y. Cai), [yji@udel.edu](mailto:yji@udel.edu) (Y. Ji).

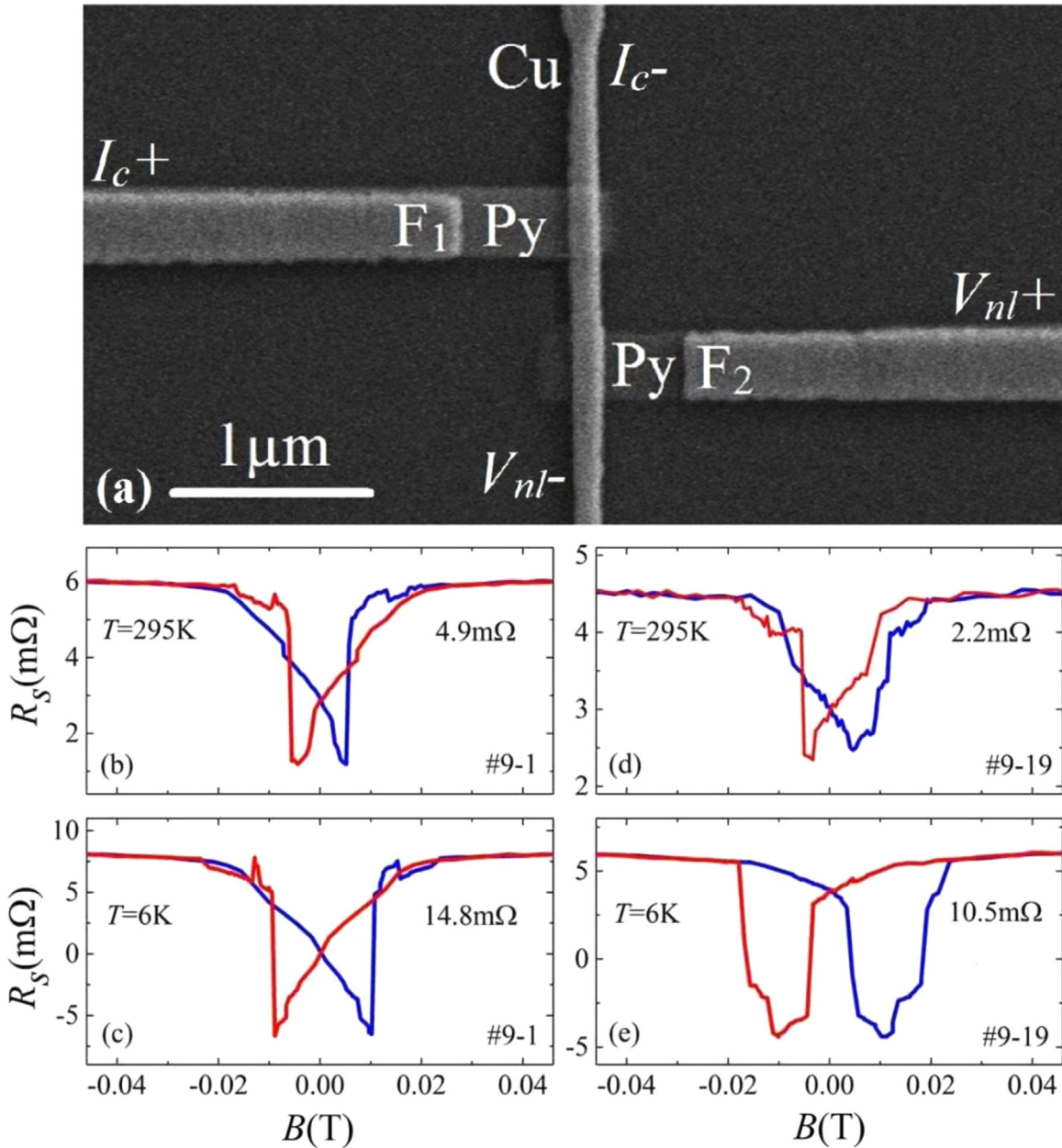


**Fig. 1.** (a) An SEM picture of an NLSV device with injector-to-detector distance of  $L=700$  nm. (b) The  $R_s$  versus  $B$  curve for device # 9-1 ( $L=400$  nm) at 295 K, showing  $\Delta R_s = 4.9$  m $\Omega$ . (c) The  $R_s$  versus  $B$  curve for device # 9-1 at 6 K, showing  $\Delta R_s = 14.8$  m $\Omega$ . (d) The  $R_s$  versus  $B$  for device # 9-19 ( $L=600$  nm) at 295 K, showing  $\Delta R_s = 2.2$  m $\Omega$ . (e) The  $R_s$  versus  $B$  for device # 9-19 at 6 K, showing  $\Delta R_s = 10.5$  m $\Omega$ .

$0.01\text{--}0.04 \Omega \mu\text{m}^2$ , which is much lower than that of a tunnel junction. The resistance of the Py/ $\text{AlO}_x$ /Cu interfaces for our NLSVs is therefore estimated to be  $0.2\text{--}0.8 \Omega$ . As we show later, the low-resistance oxide barriers can mitigate the spin resistance mismatch [19] between the Py and the Cu and provide substantial injection (detection) spin polarizations.

The devices are labeled using the row and column numbers of the  $20 \times 20$  matrix. For example, device # 9-1 is the device in row #9 and column #1. There are 5 subgroups in each row, each consisting of 4 adjacent devices with  $L=400, 500, 600,$  and  $700$  nm. A variable temperature probe station with an electromagnet (Lakeshore EMPX-HF) is used to access each device individually. An alternating current (*a.c.*)  $I_c$  is applied between  $F_1$  and the upper end of the Cu channel as shown in Fig. 1(a). A nonlocal voltage  $V_{nl}$  is measured between  $F_2$  and the lower end of the Cu channel by lock-in method and recorded as a function of the magnetic field  $B$  (applied parallel to  $F_1$  and  $F_2$ ). At 295 K, 32 devices are measured,

and at 6 K, 46 devices are measured. All measured devices show spin signals with large magnitudes. The un-measured devices on the substrate are likely to have similar qualities.

Fig. 1(b) shows the  $R_s (=V_{nl}/I_c)$  versus  $B$  curve at 295 K for device # 9-1 ( $L=400$  nm). The spin signal of  $\Delta R_s = 4.9$  m $\Omega$  is substantial, considering that  $L=400$  nm and  $T=295$  K. The  $R_s$  versus  $B$  curve at 6 K for device # 9-1 is shown in Fig. 1(c), and  $\Delta R_s = 14.8$  m $\Omega$ . Fig. 1(d) and (e) show  $\Delta R_s = 2.2$  m $\Omega$  at 295 K and  $\Delta R_s = 10.5$  m $\Omega$  at 6 K, respectively, for device #9-19 ( $L=600$  nm). Similar measurements of  $R_s$  versus  $B$  were performed to extract  $\Delta R_s$  for other devices.

These  $\Delta R_s$  values are at least comparable to the spin signals of NLSVs with smaller junction sizes ( $100 \times 80\text{--}150 \times 120$  nm $^2$ ) but similar  $L$  distances. [13,20–23] Therefore, the spin injection is effective through these low-resistance oxide junctions with larger areas ( $330 \times 170$  nm $^2$ ). The drastic decrease of  $\Delta R_s$  with an increasing junction size, as observed in ohmic junctions, [24] is

Download English Version:

<https://daneshyari.com/en/article/1798266>

Download Persian Version:

<https://daneshyari.com/article/1798266>

[Daneshyari.com](https://daneshyari.com)